AD

DEFECT CHARACTERIZATION OF OXIDE MATERIALS FOR PYROELECTRIC DETECTOR APPLICATIONS

Final Technical Report
by

David J. Keeble

(12/99)

United States Army

EUROPEAN RESEARCH OFFICE OF THE U.S. ARMY

London, England

CONTRACT NUMBER N68171-98-M-5740

David J. Keeble

Approved for Public Release; distribution unlimited

REPORT DOCUMENTATION PAGE

Form Approved
OMB No. 0704-0188

AGENCY USE ONLY (Leave Blank)	2. REPORT DATE	3. REPORT TYPE AND DATES COVERED
	22 December 1999	Final, September 1998 - September 1999

TITLE AND SUBTITLE
Defect characterization of oxide materials for pyroelectric detector applications

5. FUNDING NUMBERS
N68171-98-M-5740

AUTHOR(S)
D.J. Keeble

PERFORMING ORGANIZATION NAME(S) AND ADDRESS(ES)
University of Dundee
Department of Applied Physics and Electronic & Mechanical Engineering,
Dundee DD1 4HN, Scotland

8. PERFORMING ORGANIZATION REPORT NUMBER
ERO-2F

SPONSORING/MONITORING AGENCY NAME(S) AND ADDRESS(ES)
U.S. Army European Research Office
223 Old Marylebone Road
London NW1 5TH

10. SPONSORING /MONITORING AGENCY REPORT NUMBER

SUPPLEMENTARY NOTES

12a. DISTRIBUTION/AVAILABILITY STATEMENT

12b. DISTRIBUTION CODE

ABSTRACT (Maximum 200 words)

Characterisation of atomic-scale defects in oxides with application to pyroelectric detectors has been performed. The materials studied were ferroelectric $PbTiO_3$, $(Pb,La)TiO_3$, and $(Pb,La)(Zr,Ti)O_3$ and the conducting oxide $La_xSr_{1-x}CoO_3$. Thin films have been studied using the vacancy-related defect sensitive technique positron annihilation. Variable energy positron beam (VEPB) measurements on $Pb_{1-y}La_yZr_{0.2}Ti_{0.8}O_3$ (PLZT) for y = 0.005, 0.03, 0.06 and 0.10 were performed. The variation in annihilation characteristics was compared to the results expected from defect chemistry. The first coincidence-detection VEPB measurements on PLZT films were made. Measurements on PLZT thin films, x = 0.0 and x = 0.10, processed to give different oxygen deficiencies were made and correlated with structural measurements on the films. PLZT capacitor structures with $LaSrCoO_3$ electrodes processed in oxygen deficient ambients were then studied. Again, correlation with electrical and structural characterization measurements was made.

Electron paramagnetic resonance has been used to study $PbTiO_3$. Temperature dependence of the spectrum from Mn^{4+} allowed local structure information to be inferred. Preliminary measurements on thin film PLZT layers were attempted. This formed a complementary part of the ARL program on ferroelectric materials and infrared detectors and involved collaboration with ARL and with MRCP/MICRA programs at Univ. Maryland and Brookhaven.

SUBJECT ITEMS
Positron Annihilation, Electron Paramagnetic Resonance, Defects, Impurities, Oxide Materials, Pyroelectric Materials, Ferroelectric Materials.

15. NUMBER OF PAGES

16. PRICE CODE

SECURITY CLASSIFICATION OF REPORT	18. SECURITY CLASSIFICATION OF THIS PAGE	19. SECURITY CLASSIFICATION OF ABSTRACT	20. LIMITATION OF ABSTRACT
UNCLASSIFIED	UNCLASSIFIED	UNCLASSIFIED	

SUMMARY

Characterisation of atomic-scale defects in oxides with application to pyroelectric detectors has been performed. The materials studied were ferroelectric $PbTiO_3$, $(Pb,La)TiO_3$, and $(Pb,La)(Zr,Ti)O_3$ and the conducting oxide $La_xSr_{1-x}CoO_3$. Thin films have been studied using the vacancy-related defect sensitive technique positron annihilation. Variable energy positron beam (VEPB) measurements on $Pb_{1-y}La_yZr_{0.2}Ti_{0.8}O_3$ (PLZT) for y = 0.005, 0.03, 0.06 and 0.10 were performed. The variation in annihilation characteristics was compared to the results expected from defect chemistry. The first coincidence-detection VEPB measurements on PLZT films were made.

Measurements on PLZT thin films, x = 0.0 and x = 0.10, processed to give different oxygen deficiencies were made and correlated with structural measurements on the films. PLZT capacitor structures with $LaSrCoO_3$ electrodes processed in oxygen deficient ambients were then studied. Again, correlation with electrical and structural characterisation measurements was made.

Electron paramagnetic resonance has been used to study $PbTiO_3$. Temperature dependence of the spectrum from Mn^{4+} allowed local structure information to be inferred. Preliminary measurements on thin film PLZT layers were attempted.

This formed a complementary part of the ARL program on ferroelectric materials and infrared detectors and involved collaboration with ARL and with MRCP/MICRA programs at Univ. Maryland and Brookhaven.

KEYWORDS

Positron Annihilation, Electron Paramagnetic Resonance, Defects, Impurities, Oxide Materials, Pyroelectric Materials, Ferroelectric Materials.

Table of Contents

Appendixes

Introduction

Battlefield imaging devices should, ideally, operate at ambient temperatures; technology based on pyroelectric materials is a major contender for such devices. Pyroelectrics possess a permanent electric dipole moment, a change in temperature causes a change in the magnitude of this polarization, so inducing charges on the material surfaces. This phenomenon can be utilized to make a simple device capable of sensitive detection of infrared (IR) radiation. Device performance depends not only on the performance of the pyroelectric material but on design aspects such as thermal isolation and signal amplification. It has been found that optimizing the material performance depends on (a) maximizing the pyroelectric coefficient while (b) reducing the dielectric loss. [1]

The pyroelectric effect is described in terms of a vector, the pyroelectric coefficient $\boldsymbol{p}$, given by the rate of change of $\mathbf{P_s}$, the spontaneous polarization, with temperature, $\Delta\mathbf{P_s} = \boldsymbol{p}\,\Delta T$. Theory relates the pyroelectric coefficient to the spontaneous polarization by the expression – $p = \varepsilon\beta P_s$, where ε is the dielectric constant and β a constant obtained by comparison with experiment.[2] Operation of pyroelectric devices requires chopping the input radiation to modulate the temperature change so giving a AC signal which may be detected with maximum sensitivity. The pyroelectric performance is proportional to the pyroelectric coefficient and can depend on $(\varepsilon \tan\delta)^{-1/2}$, where $\tan\delta$ the dielectric loss. The highest pyroelectric figures of merit have been observed in ferroelectric materials.

Ferroelectric material properties are strongly influenced by the microstructure, defects, compositional inhomogeneities, external fields, and domain-wall displacements. These external factors may actually control the material response.[3]For instance, the origin of dielectric loss has been attributed to defects or domain boundaries in imperfect crystals.[2] Charged atomic scale defects such as impurities or vacancy type defects can attract one another forming dipolar defects. It has been found that these result in internal bias fields that can shift and distort the ferroelectric polarization electric field hysteresis loop.[4] Very recent first principles calculations highlight the possible importance of oxygen vacancy metal impurity complexes in ferroelectrics. [5]Defects can 'lock' the local orientation of the polarization preventing full alignment on poling the material, as required in pyroelectric applications. [6]

In contrast to the situation in semiconductors, knowledge of technologically important atomic scale defects in ferroelectric materials is in its infancy. While work on $BaTiO_3$ and the related non-ferroelectric $SrTiO_3$, carried out during the past forty years, has led to a good understanding of certain impurity defects far less is known about $PbTiO_3$. It is this material, in modified form, that is used in the majority of currently emerging ferroelectric-based technologies including pyroelectric detectors. Recent work on $PbTiO_3$–related materials have shown the presence of some interesting and unexpected defect types not known in $BaTiO_3$ or $SrTiO_3$.[7,8] However, in the area of vacancy-related defects, known to be of primary importance from defect chemistry, no unambiguous chemical identifications have been made. In consequence considerable work is required to develop knowledge of these defects in Pb-based oxide materials. Further, the current trend in detector technology is to faster arrays based on thin films. Our work using variable energy positron beam methods has, for the first time, applied these atomic scale techniques to the study of defects in thin films of these materials.[9-11] We have, for instance, shown that marked changes in defect populations occur on processing in different oxygen ambients, an important device fabrication parameter.

There is a need to detect, characterize and identify defects in ferroelectrics and to correlate this knowledge with device performance to understand the mechanisms involved in

various degradation processes. The aim is to engineer materials and processes to maximize performance.

In this report the two experimental techniques used to study atomic-scale defects in ferroelectrics will be briefly introduced, experimental details will also be included. The results will then be presented on the three research areas address though the duration of this award. This will be followed by some concluding remarks and some comments on work in progress.

The work described forms part of the Army Research Laboratory program on ferroelectric materials and infrared detectors. It involved collaboration with members of ARL and with programs at University of Maryland and Brookhaven National Laboratory funded through the ARL Microelectronics Research Collaboration Program (MRCP). Close collaboration with BNL existed in the performance of positron annihilation experiments. The EPR measurements were exclusive to this ERO program as these could not be provided at ARL or at other partner sites.

Introduction to Positron Annihilation

Positron annihilation is particularly sensitive to vacancy related defects in materials. The annihilation characteristics can be obtained from Doppler broadening of the 511keV γ-ray or from a positron lifetime experiment. Both methods allow vacancy-related defects to be identified. Positron lifetime spectroscopy allows the deconvolution of several vacancy-related defect types. The Doppler broadening detection method can be used in conjunction with a variable energy positron beam which allows the positrons to be implanted to specific depths within thin layer samples. In contrast the positron lifetime measurement is confined to bulk samples > 100 μm in thickness. Positron lifetime and Doppler broadening facilities for bulk samples are under development at University of Dundee. Variable energy positron beam measurements will be carried out at Brookhaven National Laboratory in collaboration with Dr. B. Nielsen.

Positrons implanted in to solids thermalise within 10 ps and enter a Bloch state from which they can annihilate directly or they can be trapped into a localized state from which annihilation can take place on a timescale typically in the range 100 to 500 ps. A thermal positron annihilating with an electron in a solid will do so predominately via a two γ process. These resultant 511 keV annihilation γ-rays, when viewed in the laboratory frame, are Doppler broadened by the longitudinal component of the annihilation pair momentum. The pair momentum is dominated by that of the electron. The Doppler broadened γ-ray energy spectrum provides a measure of the momentum distribution of the electrons with which the positron is annihilating. Vacancy defects, due to the missing ion core, represent an attractive potential to positrons. Annihilation from such a site is more likely to occur with low momentum valance electrons. The Doppler broadened lineshape is characterised by the S-parameter which is defined to be sensitive to low momentum events. It is the number of counts in a narrow window about the centre of the spectrum divided by the total number of counts in the line, see Fig.1. In addition the electron density at the vacancy is reduced and this results in an increase in the positron lifetime over that for bulk annihilations.

An increase in S-parameter indicates an increase in the concentration of vacancy-related defects and/or an increase in the size of those defects. The technique is sensitive to defect concentrations in the approximate range $10^{15} - 10^{19}$ cm^{-3}, however, this is dependent on the specific positron trapping rate for defects involved. [12,13] The S-parameter typically increases

by 1.5-2.5 % between undefected materials and those with a saturation concentration of monovacancy type defects. The value of the saturation defect S-parameter is a characteristic of the particular defect type and material. A systematic increase in this value with vacancy defect size is observed for any particular material. The variation as a function of defect concentration is modelled for the case of a saturation S value of 1 % is shown in Fig.2.

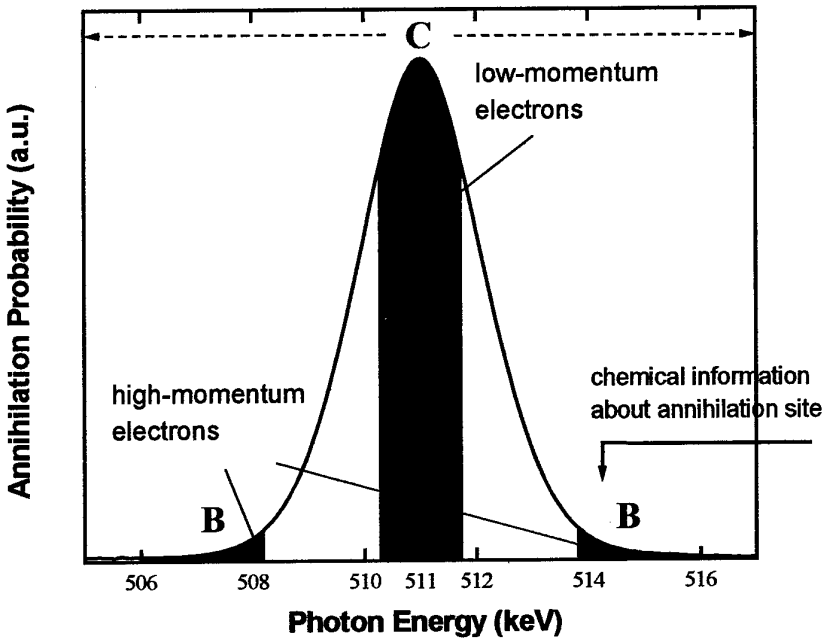

Fig. 1. Doppler Broadened 511 keV gamma-ray energy spectrum. The S parameter is defined as the counts in region A divided by the total counts in the line.

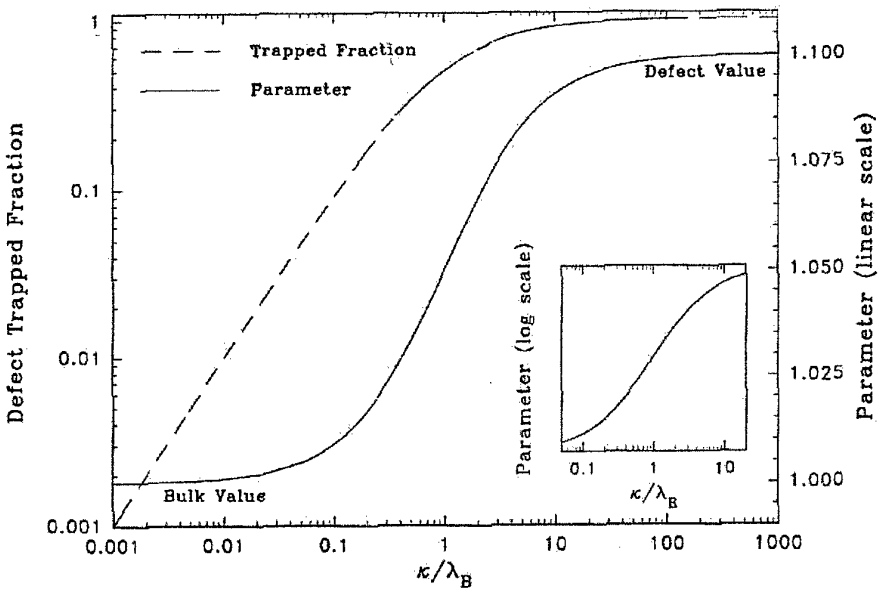

Fig. 2. Positron trapping to a vacancy-related defect as a function of concentration, c_D, with $\kappa = c_D \mu_D$ where μ_D is the defect specific positron trapping rate.

By implanting positrons into a suitable thin metal foil, e.g. tungsten, with a negative workfunction for positrons it is possible to obtain a population of thermal positrons which can then be guided and accelerated to a defined energy. This beam of monoenergetic positrons can then been implanted into a thin film and the mean depth of implantation varied by varying the positron energy. Positron annihilation can then be measured using Doppler broadening, this has the advantage of rapid data collection so allowing depth profiles to be accumulated.

Introduction to EPR

Electron paramagnetic resonance is an established technique capable of detecting paramagnetic defect states with high sensitivity. The limit is approximately 10^{11} paramagnetic centres within the sample under study. For experiments performed on solids using a typical microwave frequency in the 9 GHz band this approximates to defect/impurity concentrations of order 10^{12} cm^{-3}. Paramagnetic centres are impurities or defects that have unpaired electrons, in consequence certain charge states of metal ion impurities or native defects in solids are often paramagnetic. The spectra can be interpreted in terms of a spin-Hamiltonian.

$$H = \beta B \cdot g \cdot S + \Sigma_n \sum_{m=-n}^{m} b_n^m O_n^m + \Sigma_i \left(I_i \cdot A_i \cdot S - \mu_n g_{n,i} B \cdot I_i \right)$$

The first term is generally the dominant one, it describes the Zeeman interaction between the unpaired spin and the applied magnetic field. The spectroscopy is performed by holding the photon energy constant using a high quality factor microwave resonant cavity and sweeping the external magnetic field so altering the Zeeman splitting of the levels. At resonance microwave power is absorbed by the sample. The ability to resolve interactions with those nuclei composing the local structure of the defect or impurity and that have non-zero nuclear spin give the technique chemical specificity.

Experimental Methods

Variable energy positron beam measurements were performed at Brookhaven National Laboratory using a 0 to 30 kV accelerating potential. Positron annihilation was measured using the Doppler broadening of annihilation radiation. All thin film samples used in these studies were prepared at University of Maryland by laser ablation as part of the MRCP. Electron paramagnetic resonance measurements were performed using a 9GHz band Bruker EMX spectrometer system at University of Dundee. Progress was also made during the report period on construction of bulk sample positron annihilation facilities at University of Dundee for the collaboration, however, this work is continuing under ERO contract N68171-99-M-6463 and will be reported on fully at a later date.

Positron Annihilation Studies of La-doped PZT

The donor doping of PZT is a technologically important process. The majority of device compositions are donor doped as it has been found empirically that this gives optimal material properties. La^{3+} is assumed to substitute for Pb^{2+} and to generate cation vacancies for charge compensation. This can be expressed as

$$La_2O_3 + 2(Pb^{2+}) = 2(La^{3+})^{\bullet} + (V_{Pb})'' + 3PbO, \qquad \text{Eq. 1}$$

with $^{\bullet}$ representing positive charge and $'$ negative charge. This predicts that the material has stoichiometry $Pb_{1-(3x/2)}La_x\square_{x/2}(Zr_{0.2}Ti_{0.8})O_3$. However, an alternative reaction can occur if the material contain oxygen vacancies. In this case the oxygen carried with La_2O_3 annihilates these vacancies and charge balance is maintained, as shown below.

$$La_2O_3 + 2(Pb^{2+}) + (V_O)^{\bullet\bullet} = 2(La^{3+})^{\bullet} + (O^{2-}) + 2PbO. \qquad \text{Eq. 2}$$

It is assumed the improved properties are due, in whole or part, to these processes. Further, it is not currently possible to determine if these reactions are applicable to thin films, and if so which is dominate when using a given growth method and conditions. Traditional methods of defect chemistry are not applicable to low mass/volume samples. To compare these predictions with the positron annihilation experiments we would like to have a method of determining the chemical nature of the positron trapping site and we also need to know the specific positron trapping rate to particular defects. This is not yet possible, however, if we assume the results obtained above as a function of La content are due to trapping to lead monovacancies we are able to infer an estimate for vacancy concentration or a value for the specific trapping rate.

Variable energy positron beam (VEPB) measurements were performed on $Pb_{1-y}La_yZr_{0.2}Ti_{0.8}O_3$ (PLZT) samples with y = 0.005, 0.03, 0.06, and 0.10. Positron annihilation was monitored by measuring the Doppler-broadened γ-ray energy spectrum, the lineshape is characterised by the S-parameter. The results are shown in Fig. 3 below. The PLZT layer thickness was nominally 300 nm. The variation in S parameter as a function of La content is more clearly shown in Fig. 4. The S-parameter is seen to reach a saturation value in the region of La content x = 0.10, consistent with trapping to a neutral or negative charge state vacancy defect with a concentration that increases with increasing La content.

The assumption that the increase in S is due to the increase in concentration of a single vacancy-related defect is further strengthened by the behaviour shown in Figure 5. Here the S parameter for the layer is plotted against the W parameter for the different La-content films, the W, or wing, parameter is defined as the number of counts in the wing region (region B Fig. 1) of the spectrum divided by the total number of counts. It has been found in other systems that the S to W parameter ratio can be characteristic of particular defect types. The observation that the ratio for all the films studied forms a linear plot is evidence that the nature of the positron trap is not changing with La content, only its concentration is varying.

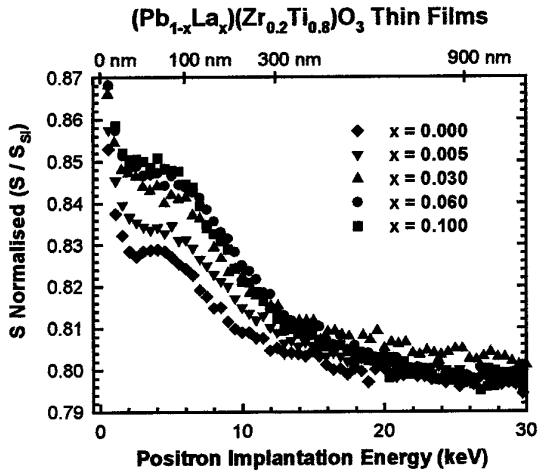

Fig. 3. S parameter depth profiles for La doped $Pb_{1-y}La_yZr_{0.2}Ti_{0.8}O_3$ (PLZT) for y = 0.005, 0.03, 0.06, and 0.10.

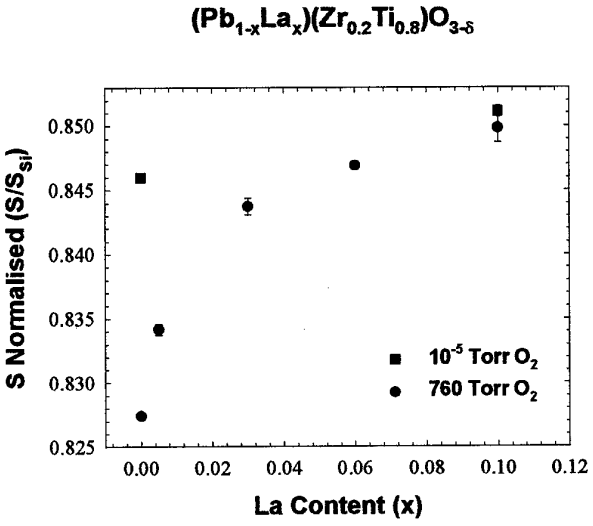

Fig. 4. S parameter for the $Pb_{1-y}La_yZr_{0.2}Ti_{0.8}O_3$ (PLZT) layer. Also shown are the results for two films cooled from the growth temperature in an ambient of 10^{-5} torr oxygen.

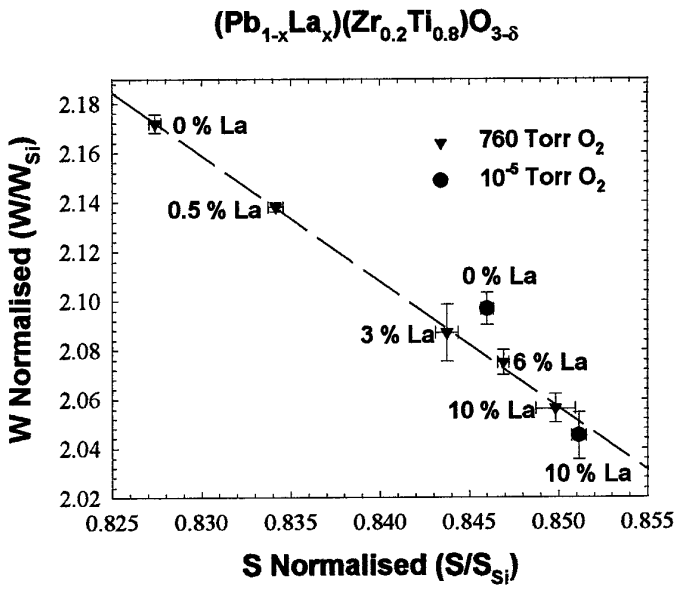

Fig. 5. W parameter against S parameter for the PLZT layer as a function of La content.

This would seem fully consistent with the defect chemistry presented earlier. An increase in La content should result in an increase in lead vacancy concentration. The cation vacancy is expected to be negatively charged and so should be a strong positron trap. However, the *S*–parameter is sensitive to changes in $\kappa\tau_b$ for the range ~ 0.1 to 10, see Fig. 2, and since $\kappa = \mu_D c_D$, where μ_D is the defect specific trapping rate (s^{-1} at.) and c_D is the defect concentration (at.$^{-1}$) this can be used to estimate defect concentrations, or defect specific trapping rates from the experimental data. From positron annihilation lifetime measurements on oxide materials an estimate of the bulk lifetime of order 200 ps can be made. The S-parameter behaviour shown in Fig. 4 suggests saturation is starting to occur at 6% La content, *i.e.* $\tau_b\mu_D c_D = 10$. Assuming Eq 1 applies this would infer a lead vacancy concentration of $c_D = 0.03$ at^{-1}. From this value the specific defect tapping rate can be estimated to be $\mu_D = 1.7 \times 10^{12}$ s^{-1} at. However, this value is orders of magnitude lower than the rates observed for semiconductors which, for negatively charges monovacancies are typically of order 10^{15} s^{-1} at.[14] If this value for μ_D is used the calculated vacancy concentration reduces to 5×10^{-5} at.$^{-1}$. Further work is in progress to resolve this inconsistency.

To provide information on the chemical nature of the positron trapping vacancy in PLZT a new experimental method was instigated at Brookhaven, coincidence Doppler detection of positron annihilation. The wing regions of the Doppler broadened energy spectrum shown in Fig.1 are formed from annihilations with high momentum electrons. These are typically due to tightly bound core electrons residing on the atoms surrounding the vacancy. Conventional Doppler broadened spectra do not have sufficient signal to background in these wing regions to resolve features, however, orders of magnitude improvements can be obtained by collecting only those gamma events where two 511 keV photons appear in coincidence.

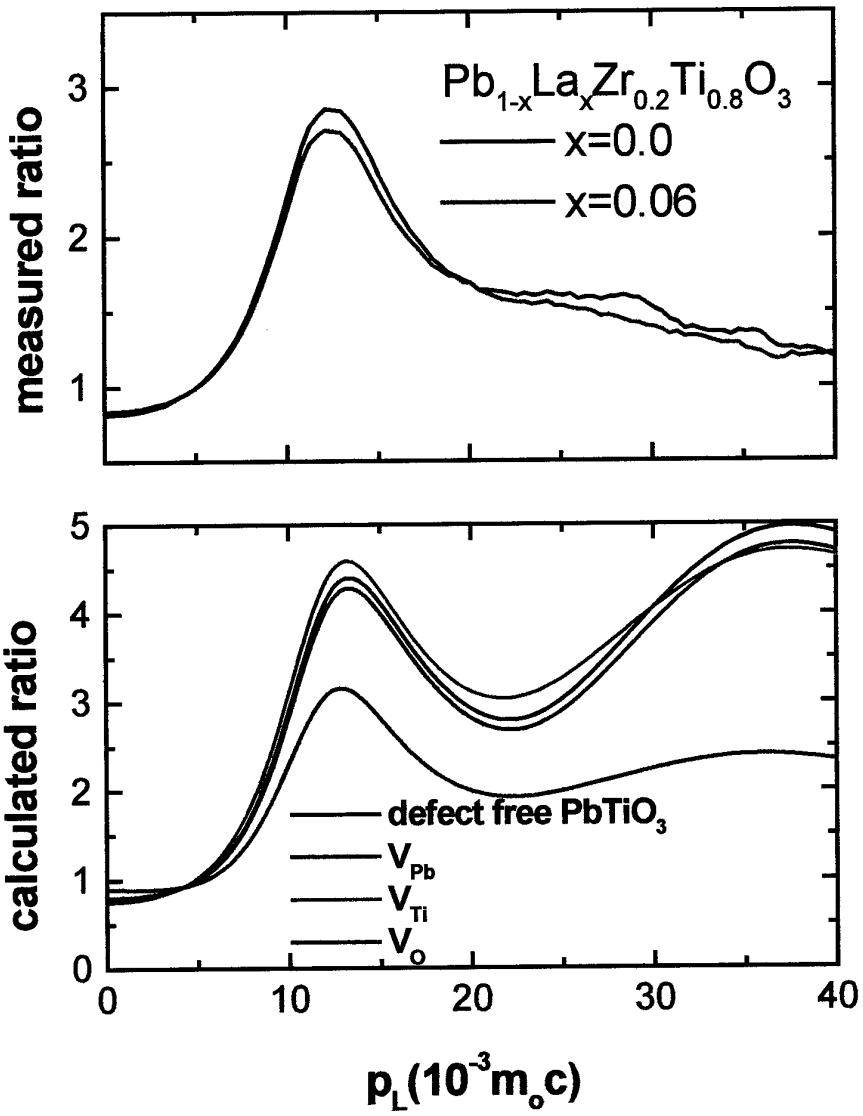

Fig. 6. Upper panel – measured coincidence Doppler spectra from PLZT. Lower panel – calculated high momentum ratio curves for vacancy defects in lead titanate.

The features present in these high momentum regions are best presented in terms of a ratio with respect to a well characterised standard, typically silicon. The technique holds the prospect of allowing chemical identification of the vacancy type, Gosh *et.al.*[15] have recently calculated theoretical difference curves for vacancy defects at the three atom sites in $PbTiO_3$ (see Fig. 6 lower panel) and show that lead vacancies should be detectable. The results of preliminary experiments on PZT thin films with 0 and 6 % La content are shown in Fig. 6 upper panel. While there is evidence of a feature in 30-40 mrad region it is very weak even in the 0 % sample. Further experiments are in progress.

In summary positron annihilation has shown there is an increase in vacancy-related defect concentration with increasing La content. However, interpretation of the increase is hampered by uncertainty in the specific trapping rate for neutral and negative charge state monovacancies in perovskite oxides. Preliminary coincidence Doppler measurements have shown sensitivity over the range of the momentum necessary for defect identification. Further systematic experiments are underway with the aim of identifying the site of the vacancy acting as a positron trap using this method combined with comparison to theory. If the positron traps can be identified and the magnitude of the positron trapping rate determined then the contributions made by Eq 1 and Eq 2 in these thin film samples could be estimated.

Positron Annihilation Studies of oxygen deficiency in LSCO/PLZT/LSCO structures

Integration of PZT devices will likely expose the materials to reducing environments so it is of interest to investigate the effect of oxygen partial pressure on the vacancy-related defect population. Measurements have been made on PLZT thin films, with La contents x = 0.0 and x = 0.10, cooled from the growth temperature under either 10^{-5} or 760 Torr oxygen, see Fig. 7 (also Fig. 4). A significant increase in S was observed for x = 0.0 and for x = 0.10, despite the positron S-parameter showing near saturation, an increase in S with the introduction of oxygen deficiency was observed. This is consistent with the modification of positron trapping sites by the addition of local oxygen vacancies and/or additional trapping at oxygen vacancy cluster sites. It should be remembered that the isolated oxygen vacancy is expected to be positively charged and so should not trap positrons.

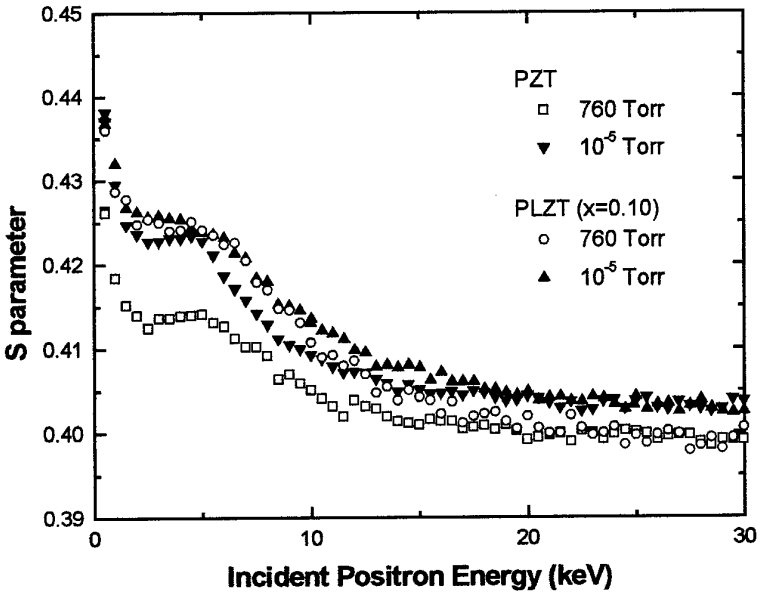

Fig. 7. S parameter as a function of incident positron energy for the PZT thin films with 0 and 10 % La contents exposed to either 760 or 10^{-5} Torr oxygen partial pressure during cooling from the growth temperature.

The conducting oxide $La_{1-x}Sr_xCoO_{3-\delta}$ (LSCO) with x = 0.5 is an important electrode material for a number of metal oxide device technologies. Here we are interested in evaluating suitability as a radiation absorbing top electrode for pyroelectric detectors. The focus of the work described here is to study the defect properties of these films for relevant processing conditions. In preliminary studies we have investigated cooling in various oxygen ambients and have applied positron annihilation characterisation.[10] This work was extended to study $La_{1-x}Sr_xCoO_3$ samples with strontium contents in the range $0.15 < x \leq 0.7$ using a 760 torr oxygen cool down. This was part of a wider programme to select the appropriate oxide electrode for the pyroelectric detector application. The positron measurements,[16] see Fig. 8, were correlated with conductivity and X-ray diffraction characterization of the films. It was found the optimal composition was again the x = 0.5.

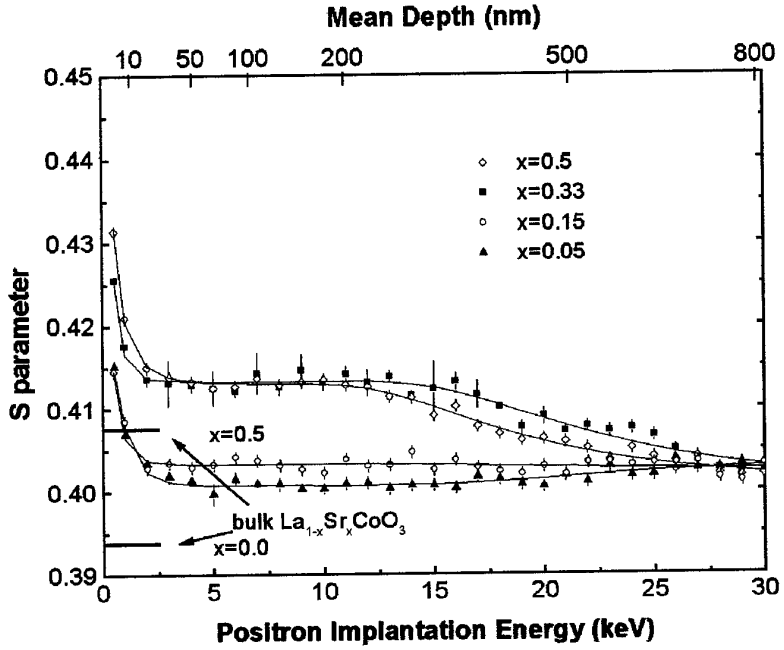

Fig. 8. S parameter as a function of incident positron energy for $La_{1-x}Sr_xCoO_3$ thin films with varying Sr contents.

The appropriate device structure for pyroelectric detectors is a simple capacitor. As described previously, the highest material quality can be obtained when conducting oxide electrodes are used. The work outlined above was extended to measure the vacancy-related defect profiles within fabricated capacitor structures. Preliminary measurements have been reported.[11] Further measurements were made on capacitors for which electrical characterisation was also performed. Two sample sets, A and B, were grown with nominal thickness of 100/300/100 nm and 40/180/180 nm, respectively. Each set consists of a pair of samples, a reference fully oxygenated sample, exposed to 760 Torr O_2 during processing, and an oxygen deficient sample, exposed to 10^{-5} Torr O_2. The samples of set A were cooled from the growth temperature at a rate of 5 K/min with the appropriate oxygen ambient. The samples of Set B were first held at the growth temperature in the oxygen ambient for 1 hr before cooling, again at a rate of 5 K/min. In Figure 9 VEPB measurements on the Set A capacitors are shown, those from Set B are presented in Figure 10.

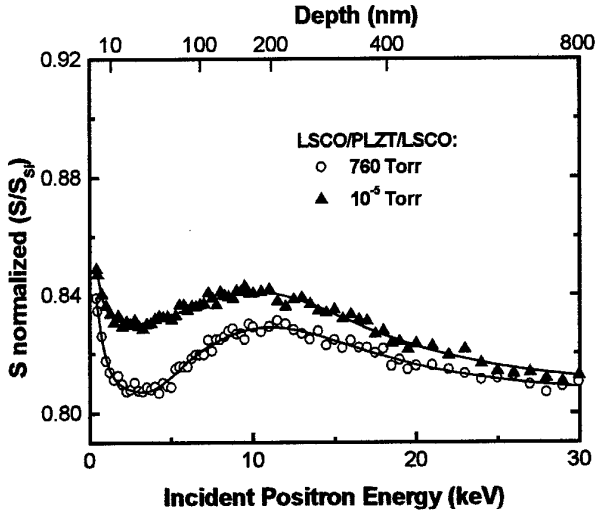

Fig. 9. S parameter as a function of incident positron energy for the LSCO/PLZT/LSCO capacitors, Set A. An approximate depth scale is shown. The solid triangles represent capacitor cooled under reducing conditions, open circles for the fully oxidized sample. Solid lines show the fit to the data using VEPFIT.

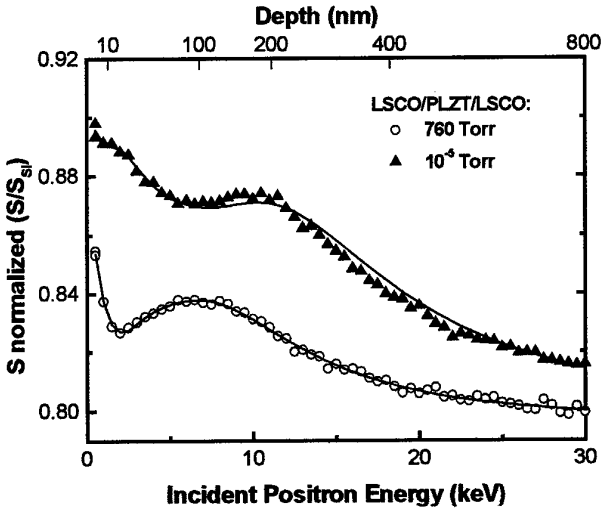

Fig. 10. S parameter as a function of incident positron energy for the LSCO/PLZT/LSCO capacitors, Set B. An approximate depth scale is shown. The solid triangles represent capacitor cooled under reducing conditions, open circles for the fully oxidized sample. Solid lines show the fit to the data using VEPFIT.

The S parameter depth profiles have been fitted using the program VEPFIT, see the solid lines in figures.[17] In this computation both the positron implantation profile and positron diffusion are taken in to account and the fractions of positrons annihilating in the individual layers is calculated as a function of incident positron energy. A superposition of layer-specific vacancy-related parameters S weighted by these calculated fractions is then fitted to the experimental data.

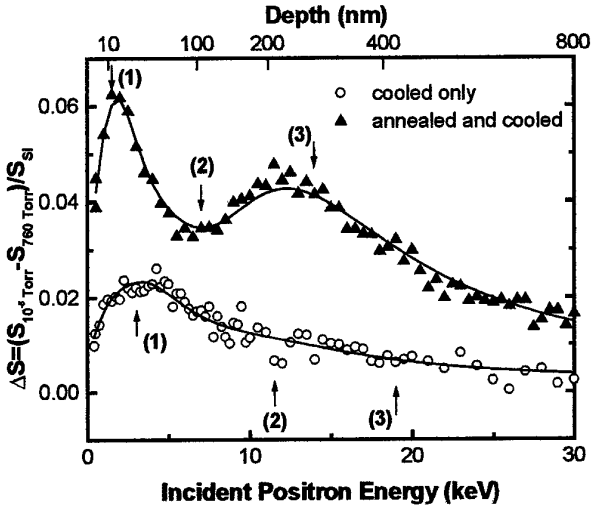

Fig. 11. S parameter difference, ΔS, profiles the LSCO/PLZT/LSCO capacitor Sets A and B. ΔS was obtained by subtracting the 760 from the 10^{-5} Torr O_2 profile. The depths at which the defect profile is a maximum for the top LSCO electrode (1), the PLZT layer (2), and the bottom LSCO electrode (3) are also shown.

Table I Fitted ΔS values for layers obtained from the positron annihilation difference profiles shown in Fig. 4 using VEPFIT.

Layer	ΔS (Set A)	ΔS (Set B)
Top LSCO	0.0124 (2)	0.034 (2)
PLZT	0.0049 (3)	0.015 (1)
Bottom LSCO	0.001 (2)	0.035 (2)

Figure 10 shows the parameter S against incident positron energy for the capacitor annealed *and* cooled in 10^{-5} Torr oxygen partial pressure together with the fully oxidized reference sample. Note the layers are substantially thinner for these capacitors so the observed changes due to oxygen non-stoichiometry are shifted to shallower depths compared to Fig. 9. The effect of oxygen deficient processing is clearly more pronounced due to the additional annealing step and the thinner top layers. This is further illustrated in Fig. 11 were the difference spectra, obtained by subtracting the defect depth profile of the fully oxidized sample from that for the oxygen deficient sample, are shown. Due to the very short positron diffusion length in these oxide layers there is negligible positron transport between layers so the resulting ΔS reflects the increase in vacancy-related defect density at the corresponding depth.

In both sample sets large changes in the open volume parameter S are observed for the top LSCO electrodes in agreement with the previously observed formation of oxygen related defects in this material. The solid curves in Fig. 11 represents a fit to the data assuming three layers on a thick substrate, each layer with a uniform defect density. The fits are satisfactory and the results are summarized in Table 1. For the sample cooled in an oxygen deficient ambient (Set A) the increase in defect density was marked in the top electrode and detectable

in the PLZT layer. However, for the sample annealed and cooled in an oxygen deficient ambient (Set B) an approximately three-fold increase in ΔS is observed for the top LSCO electrode and the ferroelectric layer compared to Set A. Further, a large increase in ΔS in the bottom LSCO electrode is found for Set B. In fact the magnitude of the increase is similar for both the top and bottom electrodes suggesting similar concentrations of oxygen vacancy-related defects are generated. These results are consistent with expected higher degree of oxygen deficiency for sample Set B subjected to the additional 1 hr anneal at the growth temperature.

Table 1 also shows that the S-parameter of the PLZT layer for this reduced capacitor has increased by 1.5 % compared to the 760 Torr O_2 cooled structure, showing that a significant vacancy-related defect concentration has formed. It should be noted electrical characterisation of this capacitor showed it to have lower polarisation value consistent with these defects contributed a significant concentration of appropriately aligned defect dipoles.

EPR Studies of single-crystal $PbTiO_3$

Electron paramagnetic resonance (EPR) is another powerful method allowing defects and impurities in ferroelectric materials to be identified and estimates of concentration made. These studies are best made using single crystal material as may EPR spectra of interest are anisotropic, this information is required to make an unambiguous identification of the centre responsible. The pyroelectric materials of interest are La doped $PbTiO_3$ and La doped $Pb(Zr,Ti)O_3$. To date relatively few EPR studies of $PbTiO_3$ have been made, this has been in part due to the lack of high quality materials. For the studies reported here crystals grown at Argonne National Laboratory by Dr. Z. Li were used. It has, so far, proved impossible to grow crystals of millimetre size of PZT or PLZT.

The aim of the work begun here is to identify both impurity and native defects in $PbTiO_3$ and to extend this to thin film $PbTiO_3$, PZT and PLZT. These initial studies have focused on Mn impurities. The EPR line positions for Mn^{4+} at room temperature are shown in Figure 12. The six line spectra are due to 100% abundant I = 5/2 Mn nucleus. The two sextets are the result of a large crystal field present at the site of the impurity. The spin-Hamiltonian that provides a satisfactory fit to the experimental spectrum is consistent with Mn^{4+} substituted at the Ti-site in the $PbTiO_3$ structure, see Figure 14.[18]

Figure 13 shows the spectrum of on of the six low field lines at 5 K. Additional superhyperfine structure is observed, this results from interactions with the near neighbour 22 % abundant I = ½ Pb nuclei. Also shown in the figure are fits obtained by assuming eight or four Pb near neighbours. This relates to the position of the impurity ion in the oxygen octahedron since, due to the ferroelectric displacement, if the ion substitutes at the true Ti site, 30 pm away from the centre, it is more nearly equidistant from the two sets of four Pb near neighbours. However, if it substitutes at the centre of the octahedron it distance between the two sets becomes unequal, see Figure 15. Thus for Mn^{4+} at 5 K the EPR spectra suggest the ion is substituted in a more nearly central position. A systematic study of the temperature dependence of the Mn^{4+} spectrum was performed, it was found that the magnitude of the crystal field at the ion site passed though a maximum in the region of 180 K, see Figure 16. The temperature dependence of the lattice parameters is monotonic hence the observed maximum suggests a local rearrangement of the impurity ion site. This is further evidenced by the temperature dependence of the superhyperfine structure, see Figure 17. Simulation of this shfs shows that the 200 K spectrum can not be fitted to four near neighbour lead ions, a more satisfactory fit is given using eight near neighbours.

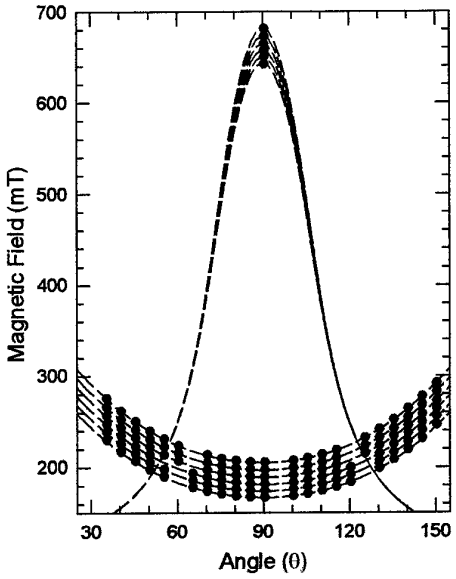

Fig. 12. $PbTiO_3$:Mn^{4+} EPR line positions as a function of the angle between the c-axis and the external magnetic field recorded at 300 K for a microwave frequency of 9.445 GHz together with the simulated line positions derived from the spin-Hamiltonian.

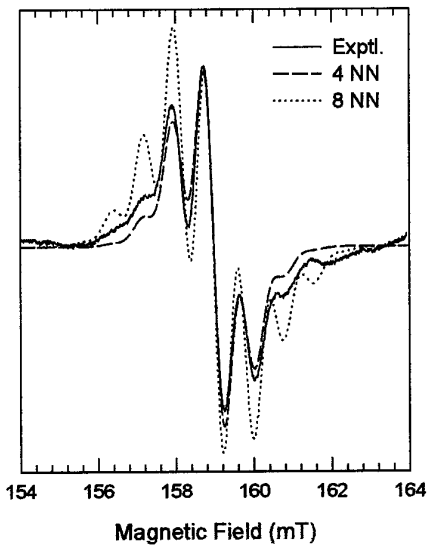

Fig. 13. $PbTiO_3$:Mn^{4+} EPR spectrum at 5 K of the $M_I = -\frac{5}{2}$ transition of the low field sextet showing superhyperfine structure. Simulated EPR spectrum assuming four and eight equidistant near neighbours lead ions are also shown.

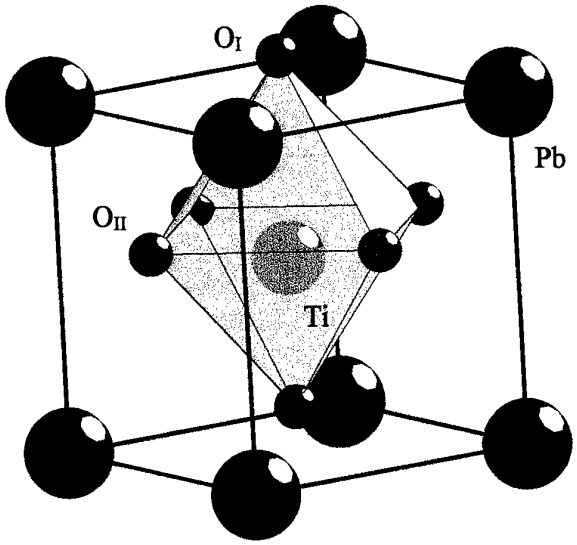

Fig. 14. Crystal structure of $PbTiO_3$.

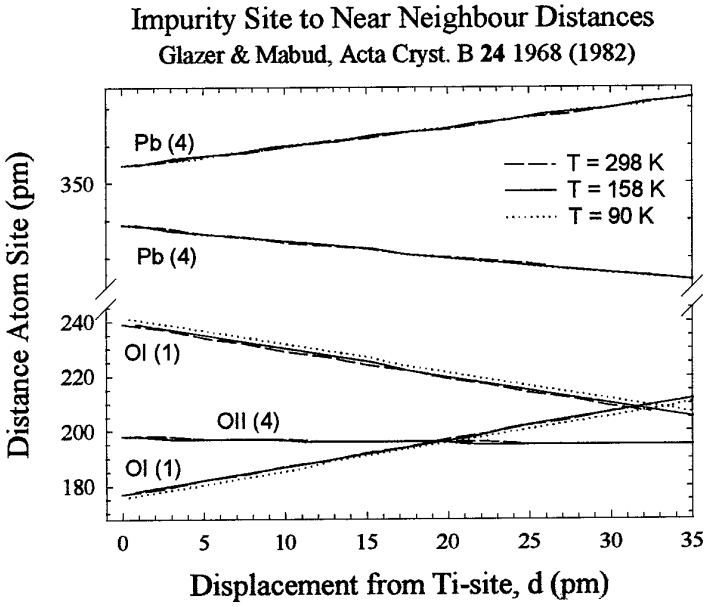

Fig. 15. Distance from impurity site position, measured with respect to the Ti ion position, in oxygen octahedron to near neighbour ion sites in $PbTiO_3$.

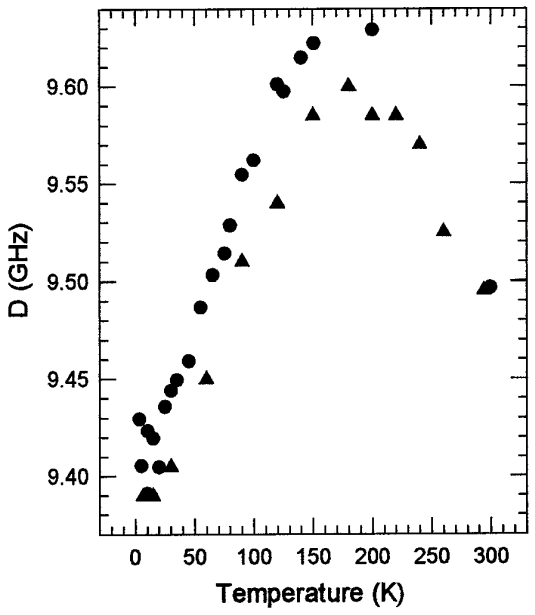

Fig. 16. $PbTiO_3:Mn^{4+}$ crystal field splitting as a function of temperature.

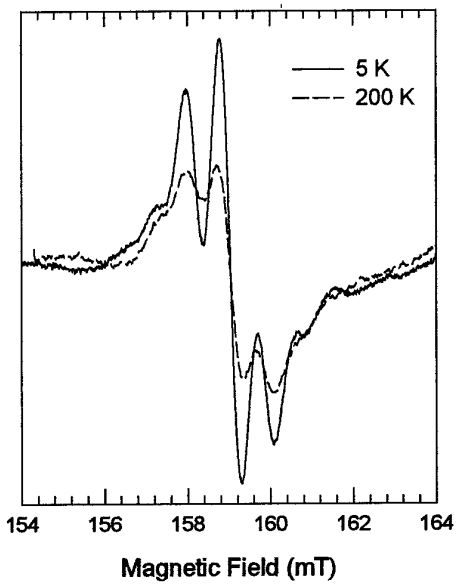

Fig. 17. $PbTiO_3:Mn^{4+}$ EPR spectrum of the $M_I = -\frac{5}{2}$ transition of the low field sextet showing superhyperfine structure at 5 and 200 K.

In summary EPR studies have initially focused on the interesting case of Mn^{4+} in $PbTiO_3$ where the technique has shown evidence of local structural sensitivity. Preliminary measurements were also completed on thin film PLZT grown on MgO substrates by laser ablation at University of Maryland, however, due to the very large impurity content in the MgO substrate no spectra attributable to the PLZT layer could be identified.

Concluding Remarks

The first measurements of vacancy-related defects in La doped PZT thin films have been made using positron annihilation. A systematic increase in positron trapping to a vacancy-related defect was observed in increasing La content. The first coincidence Doppler detected positron annihilation studies of perovskite oxide materials were performed. The technique shows potential for chemically identifying the vacancy-related defects acting as positron traps. Correlated structural, electrical and defect studies have been carried out in collaboration with Brookhaven National Laboratory, University of Maryland and ARL, Adelphi on PLZT capacitor structures similar to those to be used for pyroelectric detector applications. A correlation between the vacancy-related defect content of the ferroelectric PLZT layer and the magnitude of the polarization was found. Further the variable energy positron beam technique was found to be sensitive to changes in vacancy-related defect concentrations thoughout the structure when capacitors processed in an oxygen deficient ambient were compared to fully oxygenated structures. An increase in vacancy-related defects was also found in the bottom oxide electrode of the structure.

Electron paramagnetic resonance measurements were performed on single crystal $PbTiO_3$ and on thin film PLZT laser ablated on MgO. It was found that EPR gave detailed structural information on the site of incorporation of impurity ions in the $PbTiO_3$ structure. The preliminary measurements on thin film PLZT were unsuccessful due to the high impurity content of the MgO substrate used.

Further Work

A number of fruitful research directions have been stimulated by work reported here. A fundamental issue of the magnitude of the defect specific trapping rate into cation vacancy defects in perovskite oxides has been highlighted. Related to this, the nature of the vacancy defect acting as a positron trap in La doped PZT has yet to be unambiguously determined. To progress with these positron lifetime and coincidence Doppler detected positron annihilation studies on high quality bulk samples are planned. Positron lifetime measurements provide the ability to resolve different defect populations exhibiting distinct lifetimes but can only be routinely performed on bulk (> 10 μm) samples. Such studies on La doped $PbTiO_3$ single crystals or La doped PZT ceramic samples should allow the above issues to be resolved.

Literature cited

1. Whatmore, R. W. Pyroelectric Devices and Materials. *Reports on Progress In Physics* **49**, 1335-1386 (1986).
2. Lines, M. E. & Glass, A. M. *Principles and applications of ferroelectrics and related materials* (Oxford University Press, Oxford, 1977).
3. Damjanovic, D. Ferroelectric, dielectric and piezoelectric properties of ferroelectric thin films and ceramics. *Reports in the Progress of Physics* **61**, 1267-1324 (1998).
4. Arlt, G. & Neumann, H. Internal Bias In Ferroelectric Ceramics - Origin and Time-Dependence. *Ferroelectrics* **87**, 109-120 (1988).
5. Pöykkö, S. & Chadi, D. J. Dipolar Defect Model for Fatigue in Ferroelectric Perovskites. *Physical Review Letters* **83** 1231-1234 (1999).
6. Pike, G. E., Warren, W. L., Dimos, D., Tuttle, B. A., Ramesh, R., Lee, J., Keramidas, V. G. & Evans, J. T. Voltage Offsets In (Pb,La)(Zr,Ti)O-3 Thin-Films. *Applied Physics Letters* **66**, 484-486 (1995).
7. Warren, W. L., Seager, C. H., Dimos, D. & Friebele, E. J. Optically Induced Absorption and Paramagnetism In Lead Lanthanum Zirconate Titanate Ceramics. *Applied Physics Letters* **61**, 2530-2532 (1992).
8. Warren, W. L., Tuttle, B. A., McWhorter, P. J., Rong, F. C. & Poindexter, E. H. Identification Of Paramagnetic Pb-(+3) Defects In Lead Zirconate Titanate Ceramics. *Applied Physics Letters* **62**, 482-484 (1993).
9. Krishnan, A., Keeble, D. J., Ramesh, R., Warren, W. L., Tuttle, B. A., Pfeffer, R. L., Nielsen, B. & Lynn, K. G. Vacancy Related Defects In Thin-Film Pb(ZrTi)O_3 Materials. *Mat. Res. Symp. Proc.* **361**, 129-134 (1995).
10. Keeble, D. J., Krishnan, A., Friessnegg, T., Nielsen, B., Madhukar, S., Aggarwal, S., Ramesh, R. & Poindexter, E. H. Vacancy defects in thin-film La0.5Sr0.5CoO3-delta observed by positron annihilation. *Applied Physics Letters* **73**, 508-510 (1998).
11. Keeble, D. J., Nielsen, B., Krishnan, A., Lynn, K. G., Madhukar, S., Ramesh, R. & Young, C. F. Vacancy defects in (Pb, La)(Zr, Ti)O-3 capacitors observed by positron annihilation. *Applied Physics Letters* **73**, 318-320 (1998).
12. Dupasquier, A. & Mills jr, A. P. *Positron Spectroscopy of Solids* (IOS Press, Amsterdam, 1995).
13. Krause-Rehberg, R. & Leipner, H. S. *Positron Annihilation in Semiconductors* (Springer-Verlag, Berlin, 1999).
14. Hautojarvi, P. & Corbel, C. in *Positron Spectroscopy of Solids* (eds. Dupasquier, A. & Mills jr., A. P.) 491 (IOS Press, Amsterdam, 1995).
15. Gosh, V., Friessnegg, T. & Nielsen, B. *Phys. Rev. B* **in the press** (2000).
16. Friessnegg, T., Madhukar, S., Nielsen, B., Moodenbaugh, A. R., Aggarwal, S., Keeble, D. J., Poindexter, E. H., Mascher, P. & Ramesh, R. Metal ion and oxygen vacancies in bulk and thin film La1-xSrxCoO3. *Physical Review B - Condensed Matter* **59**, 13365-13369 (1999).
17. van Veen, A., Shut, H., de Vries, J., Hakvoort, R. A. & Ijpma, M. R. in *Positron Beams for Solids and Surfaces* (eds. Schultz, P. J. & Massoumi, G. R.) 171 (American Institute of Physics, New York, 1990).
18. Keeble, D. J., Li, Z. & Poindexter, E. H. Electron Paramagnetic Resonance of Mn^{4+} In $PbTiO_3$. *Journal of Physics - Condensed Matter* **7**, 6327-6333 (1995).

Dissemination of Results

Conference Presentations

1998 Fall MRS Meeting, Boston

"Defect identification in $(La,Sr)CoO_3$ electrodes using positron annihilation spectroscopy" T. Friessnegg et al. [O4.8]

"Defect properties of $Pb(Nb,Zr,Ti)O_3$ thin films" T. Friessnegg et al. [O7.6]

"Defect studies of $(Pb,La)(Zr,Ti)O_3$ thin films" D.J. Keeble et al. [O9.7]

1999 March APS Meeting, Atlanta

"A systematic study of defects in metal oxide and ferroelectric materials using positrons" T. Friessnegg et al. [YC 03 2]

"Electron paramagnetic resonance of metal impurities in $PbTiO_3$" D.J. Keeble et al.[LC 08 7]

1999 9th European Meeting on Ferroelectricity

"EPR studies of metal impurity ions in single crystal $PbTiO_3$"D. J. Keeble & E.H. Poindexter [MO-P75]

"Vacancy related defects in $(Pb,La)(Zr,Ti)O_{3-\delta}$ thin films studied by positron annihilation" D. J. Keeble et al. [TH-O29]

1999 Fall MRS Meeting, Boston

"Defect identification inPZT using high momentum sensitive positron annihilation spectroscopy" T. Friessnegg et al. [Y16.5]

Publications

T. Friessnegg, S. Aggarwal, B. Nielsen, R. Ramesh, D.J. Keeble and E.H. Poindexter *"A Study of Vacancy Related Defects in $(Pb,La)(Zr,Ti)O_3$ Thin Films using Positron Annihilation"*, IEEE Transactions on Ultrasonics and Ferroelectrics, **in the press**

T. Friessnegg, B. Nielsen, V.J. Ghosh, S. Aggarwal, D.J. Keeble, E.H. Poindexter and R. Ramesh, *"Oxygen deficiency and vacancy formation in LSCO/PLZT/LSCO capacitors"* in Materials Research Society Symposium, **in the press**

T. Friessnegg, S. Aggarwal, R. Ramesh, B. Nielsen, E.H. Poindexter and D.J. Keeble, *"Vacancy formation in $(Pb,La)(Zr,Ti)O_3$ capacitors with oxygen deficiency and the effect on voltage offset behavior"*, Appl. Phys. Lett., **submitted**

D.J. Keeble, A.O. Tooke, G.J. Gerardi and E.H. Poindexter, *"Local structure anomaly in $PbTiO_3$ at low temperature studied by Mn^{4+} electron paramagnetic resonance"*, Phys. Rev. B., **in preparation**

D.J. Keeble, *"Electron paramagnetic resonance of Fe^{3+} in $PbTiO_3$"*, Phys. Rev. B., **in preparation**